Sains Malaysiana 52(1)(2023): 305-320
http://doi.org/10.17576/jsm-2023-5201-25

Application of 2-D Electrical Resistivity Imaging, and Induced Polarization Methods for Delineating Gold Mineralization at Felda Chiku 3, Kelantan, Malaysia

(Aplikasi Pengimejan Kerintangan Elektrik 2-D dan Kaedah Pengkutuban Teraruh untuk Menggambarkan Pemineralan Emas di Felda Chiku 3, Kelantan, Malaysia)

HUSSEIN AHMED HASAN ZAID[1], MOHD HARIRI ARIFIN[1,*], JOHN STEPHEN KAYODE[2], MOHD BASRIL ISWADI BASORI[1], MOHD ROZI UMOR[1] & SURAYA HILMI HAZIM[1]

[1]Department of Earth Sciences and Environment, Faculty of Science and Technology, Universiti Kebangsaan Malaysia, 43600 UKM Bangi, Selangor Darul Ehsan, Malaysia
[2]Department of Physics, Nigerian Army University, No 1, Gombe road, PMB 1500, Biu, Borno State, Nigeria

Received: 6 December 2022/Accepted: 4 January 2023

ABSTRACT

A geophysical survey has been carried out to assess the distribution of gold minerals at the Felda Chiku 3, Gua Musang district, Kelantan, Peninsular Malaysia. A 2-D geo-electrical resistivity imaging (ERI), combined with Induced Polarization (IP) method, and Oasis Montaj modelling were applied to delineate the potential conductive zones associated with sulphide mineralization. Most Peninsular Malaysia's gold deposits occur in hydrothermal sulphides as discrete ore formations within the host rocks. A good correlation between the ERI and the IP profiles was observed during the interpretation of the model that successfully identifying the low resistive, and high chargeable sulphide zones, which correspond to the gold mineralization zones. The correlations could be linked to the conductive features at depth ranging from about 25 m - 135 m, trending along N-S directions. The study suggests further geo-electrical investigation to be carried out towards the south-western part of the area as more potential mineralized zones with N-S trends could be found in this region. Further studies would be able to give the extent of the gold deposits in Kelantan and by extension, allow for better informed mineral exploration and drilling operations to mine the gold in the region.

Keywords: Gold mineralization; IP chargeability method; Kelantan, Peninsular Malaysia; 2-D resistivity technique

ABSTRAK

Suatu tinjauan geofizik telah dijalankan bagi menilai taburan galian emas di Felda Chiku 3, daerah Gua Musang, Kelantan, Semenanjung Malaysia. Pengimejan kerintangan geo-elektrik 2-D (ERI) digabungkan dengan kaedah Pengkutuban Teraruh (IP) dan pemodelan Oasis Montaj digunakan untuk menggambarkan zon konduktif berpotensi yang dikaitkan dengan pemineralan sulfida. Kebanyakan deposit emas Semenanjung Malaysia berlaku dalam sulfida hidroterma sebagai pembentukan bijih diskret dalam batuan perumah. Korelasi yang baik antara profil ERI dan IP telah diperhatikan semasa tafsiran model yang berjaya mengenal pasti zon sulfida berperintang rendah dan tinggi, yang sepadan dengan zon pemineralan emas. Korelasi boleh dikaitkan dengan ciri konduktif pada kedalaman antara 25 m - 135 m, mengikut arah aliran N-S. Penyelidikan tersebut mencadangkan kajian geo-elektrik lanjut dijalankan ke arah bahagian barat daya kawasan itu kerana lebih banyak zon mineral berpotensi dengan trend NS boleh ditemui di rantau ini. Kajian lanjut juga akan dapat memberikan tahap simpanan emas di Kelantan dan seterusnya, membolehkan penerokaan mineral dan operasi penggerudian yang lebih termaklum untuk melombong emas di rantau ini.

Kata kunci: Kaedah keberintangan 2-D; kaedah pengecasan IP; Kelantan; pemineralan emas; Semenanjung Malaysia

INTRODUCTION

Malaysia is highly endowed with potential areas for mineral resources, which has long historical record in gold exploration at various places within the country's peninsula, specifically at the Central Belt of the Peninsular Malaysia (Ariffin & Hewson 2007; Arifin et al. 2019; Chu & Santokh Singh 1986; Li et al. 2015; Yao, Pradhan & Idrees 2017). In the recent literature, the distributions

and mechanism of the Peninsular Malaysia's gold deposits in the hydrothermal sulphides have gained better understanding through the advanced, and modern geophysical exploration (Arifin et al. 2019; Kayode et al. 2022). A selected number of geophysical techniques have been applied to the study area combined with the 3-D Geographic Information System (GIS) analysis and Oasis Montaj modelling in order to thoroughly investigate the area for the potential zones for gold mineralization at the Felda Chiku 3, Gua Musang, Kelantan. The choice to use a combination of methods is to improve gold prospectivity as informed by better data quality and depth of probing. While Electrical Resistivity Imaging (ERI) is commonly deployed to investigate subsurface lithological variations, stratification, and differentiation more rapid and cost-saving method in collecting quality subsurface information for evaluation purposes needs to be considered (Arifin et al. 2020a, 2020b, 2019; Kayode et al. 2022).

Based on the geological and tectonic settings of the study area, the gold deposits in this belt have been recently classified as mesothermal lode and orogenic types (Afiq et al. 2022; Ariffin 2012; Ariffin & Hewson 2007; Makoundi et al. 2014; Yeap 1993). These deposits are dominantly hosted in low-grade volcano-sedimentary rocks with steeply dipping faults (Endut et al. 2015; Metcalfe 2013, 2000; Pour & Hashim 2015; Pour et al. 2016; Sevastjanova et al. 2011). Most of the national gold deposits are produced from Pahang and Kelantan within the Central Belt mentioned by Ariffin (2012), Ghani et al. (2009) and Kayode et al. (2022) in their studies that the structural orientation in Kelantan trends N-S to NW-SE which is believed to have originated from a post-orogenic phase.

A few research papers were published in the literature on the use of other geophysical methods for gold exploration outside of the commonly used gravity and magnetic methods by the United States Geology Survey (USGS, Doyle 1990). Gold minerals have the average density values of about 19,300 kg m^{-3}, and the electrical resistivity value of about 2.4×10^{-8} Ohm-m. Although there were low grades of the precious metallic subsurface material detectable with the application of metallic sensors in those eras, it was the presence of massive sulphides, faults, shear zones, and highly conductive or resistive materials in host rocks (commonly associated with the occurrences of economically viable subsurface minerals), which paved the way for the indirect geophysical exploration (Bayrak & Şenel 2012; Doyle 1990; Haidarian Shahri et al. 2010; Kayode et al. 2022).

The recent advancement in the prospect for gold has made many developmental projects possible, leading to economic gains in most parts of the world. The exploration mechanism for these economically enriched deposits as distributed within the Malaysia Peninsular are better understood within the eastern and western blocks of the Peninsula (Kayode et al. 2022; Yusoff, Abdul Aziz & Roselee 2022; Zhang et al. 2020). The gold mineral is in association with the phyllites, and schist rich sulphide ore as reported in Arifin et al. (2019), with interbedded stratigraphic lithologies containing both sandstones and shales rock types which dated back to the Triassic age, a member of the Telong Formation. It is very common for gold occurrences to be found under hydrothermal conditions with developmental activities that control the main deposits within the volcanogenic sulphide as the host rocks together with associated structures (Kayode et al. 2022).

In the Peninsular Malaysia gold deposit, the hydrothermal setting together with the ideal mineralization conditions that controlled the principal gold deposits in Kelantan, have been given lots of attention in the recent times (Kayode et al. 2022; Yusoff, Abdul Aziz & Roselee 2022). The propagation of massive volcanogenic sulphides through faulted planes from the Earth's interior to the surface gave rise to a completely new geological structure which is termed the 'Peninsular Malaysia Gold Belt (PMGB)'.

There have been reports of the existence of gold mineralization by the exploration team at the present study site, leading to exploration and exploitation activities within Kelantan. The discovery of the earlier researchers led to the 30 prospective gold exploration areas discovered through the application of integrated geochemical analysis, geological and geophysical assessment combined with datasets from the mining sites (Ariffin 2012; Arifin et al. 2019; Goh, Teh & Wan Fuad 2006; Kayode et al. 2022; Tagwai et al. 2019; Yusoff, Abdul Aziz & Roselee 2022). The investigated area, i.e., the Felda Chiku 3, is part of the Malaysian Central Gold Belt (MCGB), and one of the enormous enrichments in potential gold deposit regions in the Peninsular, with the great prospect of abundant massive sulphide-gold rich mineralization. Several geophysical prospection approaches are based on the detection of the contrasts in diverse physical properties of subsurface materials (Telford, Geldart & Sheriff 1990). The electrical resistivity methods are applied on a continuum basis for prospecting the metallic minerals deposits associated with oxide, and sulphide minerals (Ariffin 2012; Arifin et

al. 2019; Goh, Teh & Wan Fuad 2006; Kayode, Arifin & Nawawi 2019; Moon, Whateley & Evans 2006; Sumner 1976; Tagwai et al. 2019). The zones with recorded both low resistivity/high conductivity and high chargeability enclosed the massive sulphide gold mineral with a higher percentage of concentration (Gouet et al. 2013; Kayode et al. 2022).

The objective of this study was to analyse the geophysical signature of the massive Felda Chiku 3 gold mineralization, using integrated electrical methods. The results of this study have provided sufficient information and discussion to improve gold mineral prospectivity, the data quality and the depth of probing by the deployed methods.

The ERI and IP, collectively known as the geoelectrical techniques deployed have capability of complementing each other for rapid subsurface assessment of the target's zones using the electrical resistivity and chargeability to locate the subsurface structures, depths, and the lateral spread of the lithological strata. As a result of the successes, the methods have been used to characterize the underground geological structures in multiple ways, as well as prospecting for valuable and economically, and naturally endowed resources, as well as providing long-term solutions to geohazards and environmental issues. Several researchers have developed varieties of electrode array combinations to produce successful results from the data analysis. Recently, Arifin et al. (2019) and Kayode et al. (2022), applied the techniques to prospect for gold mineralization, which served as catalyst to the present research work. In the same way, Sono et al. (2020), recently combined the ERI and IP, to delineate zones of potential gold mineralization in the Mopolo area of Southeast Botswana, Africa. On the other hands, Moreira, Casagrande and Borssatto (2020) deployed the IP and DC (direct current) resistivity methods for long-term mine planning in a sulphide deposit in Brazil. Similarly, Mashhadi, Nikfarjam and Mehrnia (2020) also applied IP and resistivity to reinterpret the data to explore gold mineralization zones at Zarzima in Iran. The technique was recently used by Kayode, Arifin and Nawawi (2019), to propose a suitable location for the Quarry industry. The technique, when integrated, could be utilized in diverse ways to characterized the subsurface structures (Arifin et al. 2020a, 2020b; Fon, Che & Suh 2012; Irvine & Smith 1990; Kayode et al. 2019; Keary & Brooks 1991; Lenhare & Moreira 2020; Mashhadi & Ramazi 2018; Moreira et al. 2016; Salarian et al. 2019; Spitzer & Chouteau 2003; Sultan et al. 2009; Vieira et al. 2016; Wynn & Grosz 2000).

GEOLOGICAL SETTING

REGIONAL GEOLOGY

Malaysia is a highly endowed region with varieties of mineral resources and has long historical record in gold mining at various places within the Central Belt of Peninsular Malaysia (Arifin et al. 2019; Ariffin & Hewson 2007; Chu & Santokh Singh 1986; Li et al. 2015; Yao, Pradhan & Idrees 2017). Based on the geological and tectonic settings, the gold deposits in the Central Belt are classified as mesothermal lode and orogenic types (Ariffin 2012; Ariffin & Hewson 2007; Makoundi et al. 2014; Yeap 1993). These deposits are dominantly hosted in low-grade volcano-sedimentary rocks and associated with steeply dipping faults (Ariffin 2012; Endut et al. 2015; Pour & Hashim 2015; Pour et al. 2016).

More recently, the distributions and mechanism of the Peninsular Malaysia's gold deposits in hydrothermal sulphides have gained better understanding through the results obtained from advanced and modern geophysical exploration methods (Arifin et al. 2019), resulting in an introduction of new gold prospectivity mapping in Peninsular Malaysia gold deposits distribution.

STUDY AREA

Most of the Peninsular Malaysia gold resources are prominently mined in the state of Pahang and Kelantan which lie within the Central Belt (Ariffin 2012). Within the Kelantan, there is a total of 30 prospective gold areas that were identified by the integrated assessment with the application of geological, geochemical, geophysical, and mining data (Ariffin 2012; Arifin et al. 2019; Goh, Teh & Wan Fuad 2006; Kayode et al. 2022; Tagwai et al. 2019; Yusoff, Abdul Aziz & Roselee 2022). It was also proposed that the Ag-Au quartz veins served as the most important gold enrichment mineralization mechanism in Kelantan area (Ariffin 2012; Arifin et al. 2019; Kayode et al. 2022; Tagwai et al. 2019).

The study area is located at Felda Chiku 3, between latitudes 4° 56' 40" N and 5° 3' 20" N and longitudes 102° 5' 0" E and 102° 11' 40" E, (Figure 1). It is about 40 km to the Gua Musang district, and at about 10 km from Kampung Paloh 2, in the southern part of central Kelantan, Peninsular Malaysia. The area is accessible by the Kota Bharu - Gua Musang Highway and characterized by hilly topographic terrains gridded by the West Malaysia, Rectified Skew Orthomorphic (RSO), using the Kertau 1948 Datum system with an average altitude ranging from 100 to 320 m above mean sea level (MSL). The land-use is composed of forest, and mostly

covered by palms and rubber trees, hence, exposure of the country rocks is minimal. The study area enclosed Sungai Galas from the confluence of Sungai Chiku, and the upstream of Sungai Galas.

The study area is underlain by sedimentary rocks of Permian and Triassic ages (Arifin et al. 2019). The Triassic rocks comprises of predominantly argillaceous-arenaceous sedimentary rocks with the Permian volcanic-sedimentary, and limestone intercalations (Goh, Teh & Wan Fuad 2006; Macdonald 1967; Yao, Pradhan & Idrees 2017). The argillaceous-arenaceous sequences observed in the field consists of the phyllites, lapilli tuffs and schists, and majority of the rocks are cross-cut by quartz veins (Figure 2). The existence of gold deposits

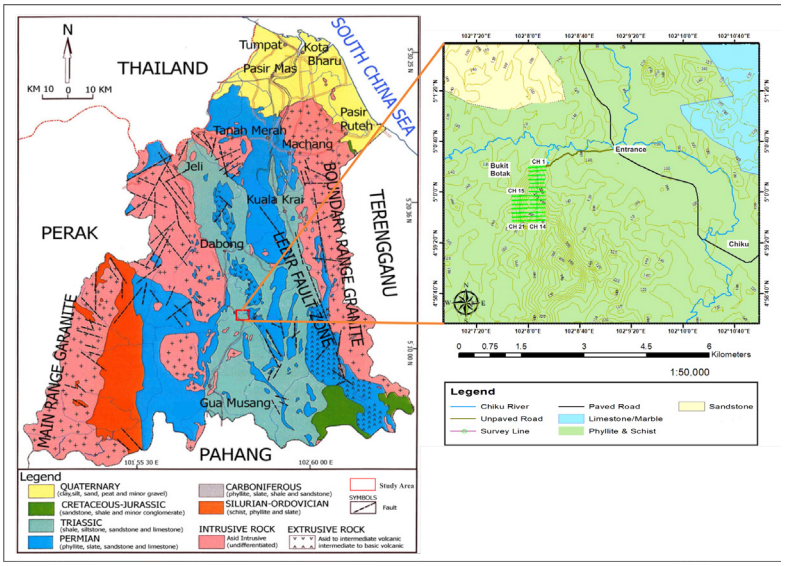

FIGURE 1. Geological map of the study area (right side), and location of Kelantan (left side), modified from Nazaruddin et al. (2015)

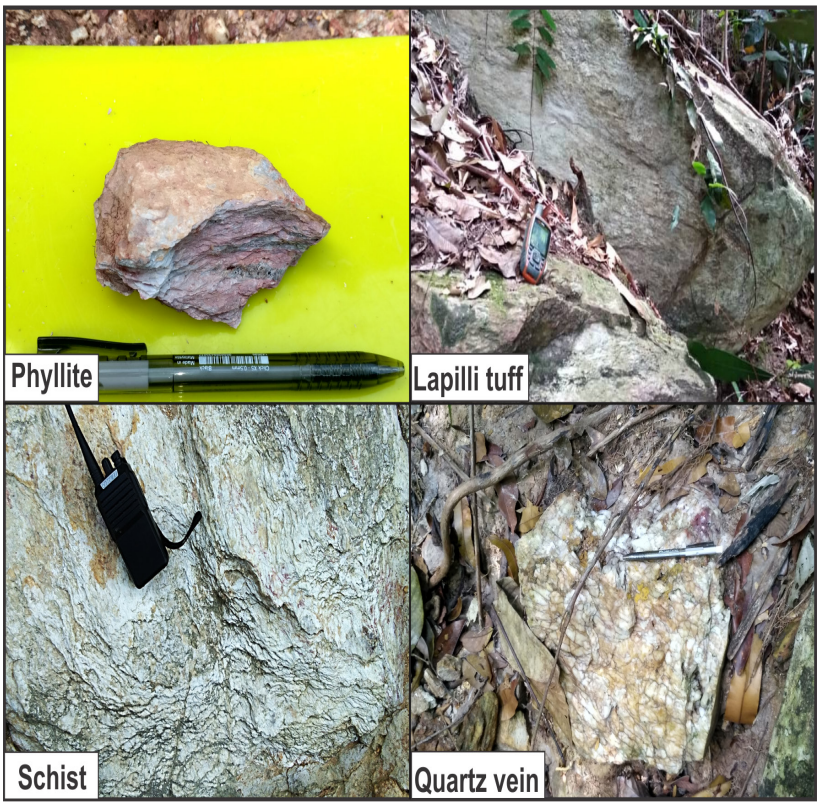

FIGURE 2. Types of rocks exposed within the study area as observed during the field survey with the quartz vein showing at the right bottom panel

in the area is reported to be associated with quartz veins containing low and high sulphides hosted in the sedimentary rocks and sheared granitoid (Arifin et al. 2019; Goh, Teh & Wan Fuad 2006; Kayode et al. 2022).

The Peninsular gold deposits at the study area are primarily controlled by the hydrothermal conditions and mineralization processes that are rich in modern and ancient volcanogenic massive sulphides that also includes low sulphide and high sulphide quartz veins that mutually occurred with quartz veins within sheared granitoid to the exterior ground, thereby creating the new geological structures as huge sulphides that are referred to as 'the gold deposits' (TGD) in these regions (Arifin et al. 2019; Kayode et al. 2022). The mineral composition of the sulphide is by and large, near to the ground surface (shallow), and limited to an area that is not too extensive. The region was reported to have high mercury and silver contents which could perhaps be due to the location of an intrusion that possibly be at depth of about 700 m below the ground surface. Field observations of the area during the field mapping, showed varied lithologies that are primarily made up of the lapilli tuff, the phyllites, and schist formations as indicated on the geological map after Arifin et al. (2019). The majority of the phyllites and the schists enclose the quartz veins. In contrast, the quartz veins were delineated alongside the foliated host rocks, the fissures, and fractures within the schists, and the phyllites formations.

Methods

To achieve the primary objective of this study, twenty-one (21) parallel resistivity and IP survey lines were deployed in an east-west directions using pole-dipole configurations to pinpoint promising zones for drilling, as this method provides a good compromise between signal strengths and spatial resolution images (Dahlin & Zhou 2004). Induced polarization imaging is an appropriate option for gold delineation as it is reported as a useful approach for mineral exploration (Flores & Peralta-Ortega 2009; Kayode et al. 2022; Sumner 1976; Telford, Geldart & Sheriff 1990; Upadhyay et al. 2020). Electrical resistivity measurement was used along all survey lines to visualize the subsurface geological structures.

The solutions to subsurface lithological stratum geological complications may perhaps not be single-handedly solved by one specific geophysical tool. In many cases of geophysical exploration, an integrated approach is the most common way of validating the results with true ground geological datasets (Arifin et al. 2019; Kayode et al. 2022). Identification of gold mineralized deposits in the field have been given priority in this study as detailed studies surrounding gold prospectively continue to gain interest and traction in many countries of the world driven by the high prices of gold worldwide.

Data Acquisition

To obtain the ERI properties of the subsurface geological lithologies, a direct current (DC) supplied by a battery with 30 Amp-hour capacity to the ABEM Terrameter SAS4000 resistivity meter arrangement with inbuilt microprocessor, coupled with multi-core 100 m cables length through copper connecting jumpers connections to the 41 and 61 stainless steel metal electrodes driven to the ground with sufficient length to pass the current at 100 mA into the ground, and the resulting potential difference measured across the potential electrodes, to give the electrical properties of the subsurface lithological units in form of apparent resistivity and apparent chargeability respectively. Another circuitry selector unit, i.e., the ABEM LUND ES 10 - 64C, was used to control the electronic switching unit to automatically select the four relevant electrodes for each of the measurement at a time.

The geophysical survey uses integration of ERI, and IP measurements applied along twenty-one (21) profiles at 5 m and 10 m, respectively, that covered an approximate ground surface distance of about 8.40 km, representing a substantial coverage of the area, were acquired to provide the desired geoelectrical data for the gold mineral prospection (Figure 3). The data helped to delineate, and map the potential of gold mineralization within the massive sulphide gold deposits in the southern region of central Kelantan, East Coast of the Peninsular Malaysia, using the Pole - Dipole electrode configurations to get the maximum depth of about 150 m with 400 m length of electrode spreads, due to its general advantages of better lateral and vertical resolution, together with its higher signal-to-noise (S/N) ratio, which is crucial to obtaining higher resolution images (Arifin et al. 2020b, 2019; Kayode, Arifin & Nawawi 2019).

Electrical Resistivity Imaging (ERI), and Induced Polarization (IP), Techniques

The methods of geoelectric prospecting identify the effects of direct current passing through a material volume by means of current electrodes and record the electrical potential across the potential electrodes to acquire the electrical properties of encountered formations (Loke 2001; Smith & Sjogren 2006). The results of these techniques are based on both the configuration of electrodes, and the responses of physical properties

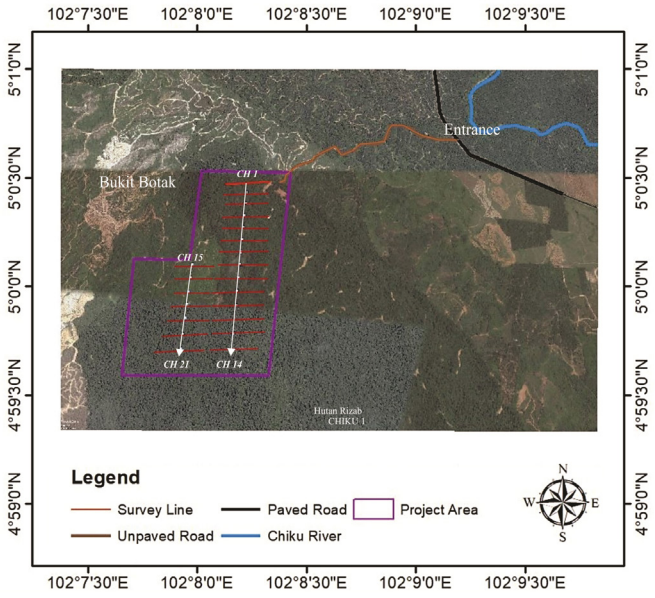

FIGURE 3. Location map of the geoelectric survey lines in the Felda Chiku 3 area, Gua Musang district of central Kelantan, East Coast, Peninsular Malaysia

to electrical current (Loke 2016; Marescot et al. 2008; Sharma 1997; Upadhyay et al. 2020).

The induced polarization also uses the same methods as that of the electrical resistivity techniques. The difference between the ERI and IP, is that the IP method measures the apparent chargeability or chargeability of the earth material, expressed in milliseconds or in millivolts per Volt (Spitzer & Chouteau 2003). When the electrical current is injected into the ground, certain subsurface units, or metallic grains (a metal sulphide), which acts as ions within rock bodies, may become electrically polarized (i.e., holds electrical charges). After the applied current is switched off, the polarized ground gradually decays with time to approach zero (Reynolds 2011). The study of voltage decay as a time function is known as the time-domain IP (TDIP). It is mainly used in the applied geophysics for mineral exploration and exploitation programme (Kumar et al. 2017; Upadhyay et al. 2020).

The host rocks association with conductive/resistive and electrically polarizable subsurface geological formations makes geophysical exploration and exploitation possible. To this effect, 2D ERI and IP geophysical survey were conducted at the Chiku 3 (CH) study site to obtain the full distributions of the electrical conductivity/resistivity and the chargeability inside these host rock bodies using the parameters presented in Table 1. The 2D ERI is a fast geophysical technique that is deployed at the ground surface for subsurface geological features surveying, and assessment of the structural features of interest. The methods adopted in this study, complemented each other for rapid measurement of the gold bearing features, through the delineation of the depths of burial, lateral extension, and accurate pinpoint of the location of quartz veins alongside the foliated host rocks, the fissures, and fractures within the schist, and the phyllite formations at the ground surface. Though the combinations of ERI and IP geophysical methods significantly help to rapidly classify the subsurface geological rock masses qualitatively, in regions with complex geological terrains, interpretation of geophysical methods may perhaps not as simple as many non-geoscientists' thoughts. Most cases of complex basement terrains possess complicated subsurface structural lithologies that require real ground surface validation of the geophysical prospection, for the improvement of the final results (Arifin et al. 2020a, 2020b).

Elevation and position for each of the stainless-steel metal electrodes were recorded using the Global Positioning System (GPS). Inverting and modelling of the field data were initially performed using RES2DINV software from Loke (2016) to display the raw data in visual models of the subsurface using the distance and generated depths, as well as topographic corrections. The inverted results were interpolated using the Oasis

Montaj software to create a 3-D voxel model following the methods in Mostafaei and Ramazi (2018).

The detail localized geology in conjunction with the subsurface structural lithologies within the subsurface of the study site was made possible to evaluate with the ERI geophysical method, whereas the IP effects was used to delineates the potential mineralized massive sulphide zones (Arifin et al. 2019). The final models obtained were in close relationship with the gold bearing massive sulphides structures. On a general note, the strengths of the ERI and IP techniques adopted for the research, were established by the inbuilt matrix evaluation in the RES2DINV software amid the mineralized zones and the geophysical models obtained. The most promising profiles from the twenty-one (21) ERI and IP were selected for the detailed reports.

The chargeability measured in the time-domain gives the IP effect that is mutually susceptible to the bulk electrolytic conduction, and the structural properties of the subsurface geological features which determined the ground surface polarization of the gold bearing mineralized sulphides. The IP effects in the interpretation of geophysical surveys could be due to lithological variations within the subsurface geologic units and also, due to the salinity of water bodies that filled up the pore spaces. However, the RES2DINV software used to normalize the chargeability due to these IP effects thereby facilitating their discriminations in large scale field-data collections. The sensitivity of the selected Pole - dipole electrode configurations was able to capture the divergence in the subsurface potentials because of the changes in the subsurface lithological geologic units (Power et al. 2018).

DATA ANALYSIS

The detailed survey parameters along each profile line with distributions of the estimated maximum depth of penetrations to the subsurface lithologic units recorded and presented in Table 1. The estimated depth of 150 m, for each of the surveyed profile enabled detailed observations of the near subsurface units to be delineated for varied data points from between $735 \leq 1403$, as recorded. The percentage RMS error varied from between 15% and 31.6%, for the RES2D data, and from between 1.1% and 23% for the IP data.

TABLE 1. Detail survey parameters along each profile line with an estimated maximum depth penetration

Date of acquisition	Survey Profile line	Length (m)	Electrode Array	Electrode spacing (m)	Estimated maximum depth penetration (m)	Data Points	RMSEC Error (%)	
							Res.	IP
5th to 7th May 2018	CH 1	400	Pole - dipole	5	150	1316	23.8	5.8
	CH 2	400	Pole - dipole	5	150	1391	28	1.6
	CH 3	400	Pole - dipole	5	150	1381	26.4	6.4
	CH 4	400	Pole - dipole	5	150	1403	18.8	4
	CH 5	400	Pole - dipole	5	150	1380	21.4	3.4
	CH 6	400	Pole - dipole	5	150	1349	15.8	1.1
	CH 7	400	Pole - dipole	5	150	1246	18.8	3.8
11th to 13th May 2018	CH 8	400	Pole - dipole	10	150	839	23.5	2.3
	CH 9	400	Pole - dipole	10	150	777	22.5	9.2
	CH 10	400	Pole - dipole	10	150	822	22.8	13.7
	CH 11	400	Pole - dipole	10	150	844	20	5.1
	CH 12	400	Pole - dipole	10	150	796	26.9	3.6
	CH 13	400	Pole - dipole	10	150	735	20.7	9.8
	CH 14	400	Pole - dipole	10	150	890	21.3	6
21st to 22nd June 2018	CH 15	400	Pole - dipole	10	150	871	20	12.1
	CH 16	400	Pole - dipole	10	150	827	21.8	6.2
	CH 17	400	Pole - dipole	10	150	808	26	7.2
	CH 18	400	Pole - dipole	10	150	866	22.9	23
	CH 19	400	Pole - dipole	10	150	794	31.6	19
	CH 20	400	Pole - dipole	10	150	853	24.2	5.7
	CH 21	400	Pole - dipole	10	150	873	20.5	5.2

RESULTS

RESISTIVITY AND CHARGEABILITY SECTIONS MODELS

Figure 4 presents the results of resistivity and chargeability inverse model obtained along the geoelectric survey line Four (i.e., CH 4). The profile gives two main low resistive zones at horizontal ground surface of between about 60 m and 115 m, and between about 140 m and 200 m, with delineated resistivity value that is less than 200 Ohm-m, extending towards the south-west downwards as indicated by the black dashed lines shown in Figure 4(a). While the resistivity responses of the surrounding host rocks, ranged between about 400-800 Ohm-m. The chargeability anomaly recorded is greater than 25 msec, at a distance of about 60 m to 120 m, within the depths range of 30 m to 90 m, associated with the low resistive zones (Figure 4(b)). The high chargeability zone recorded suggests that the sulphide mineralization zone is hosted by the quartz veins. Meanwhile, the high resistivity values greater than 2000 Ohm-m recorded, corresponds to the basement rock unit.

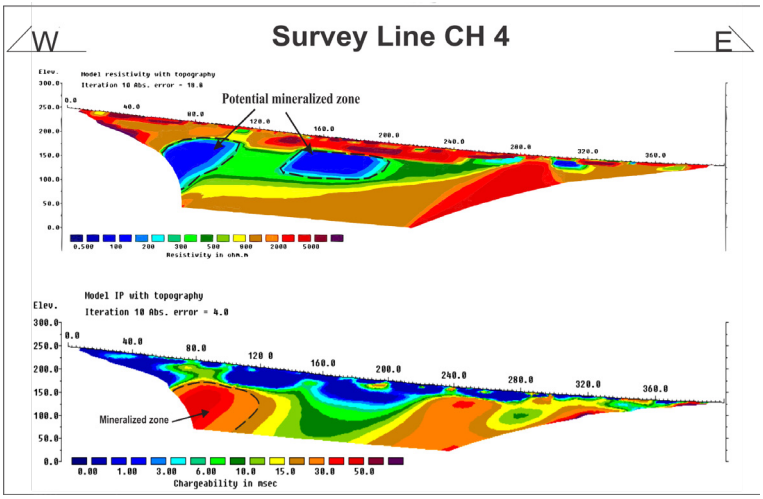

FIGURE 4. Inverted resistivity and chargeability model for the Pole - dipole electrode configuration geoelectric profile four (CH 4)

The resistivity and chargeability inverted models obtained from the geoelectric survey profile Ten, i.e., CH 10 (Figure 5), show multiple conductive subsurface anomalies at approximate distances of about 90 m, 240 m, and 320 m, respectively, with varied depths of below about 25 m down to about 110 m. The respective resistivity and chargeability values recorded for the conducting bodies are less than 200 Ohm-m, and greater than 30 msec, as presented in Figure 5(a) and 5(b), and are well correlated with the surrounding regions corresponding to the basement rocks, with respective resistivity and chargeability values that are greater than 2500 Ohm-m, and less than 10 msec.

Figure 6 shows images of the resistivity and the chargeability results for the survey line Seventeen (i.e., CH 17). In the ERI model section (i.e., Figure 6(a)), two zones of low resistive values were observed at the horizontal distance of between about 95 m and 234 m, for the first zone, and between about 240 m and 342 m, along the geoelectric survey line, with recorded values less than 250 Ohm-m. These low resistivity values correspond to the high chargeability values greater than 15 msec recorded (i.e., Figure 6(b)), at a depth of about 28 m. The zones with low resistivity are indications of the presence of conductive sulphide mineralization that hosted the hydrothermal quartz vein through the sheared zone where the gold mineral resides.

In the inverse models along the geoelectric profile Eighteen (i.e., CH 18), as presented in Figure 7. The profile delineates a considerable extension of the low resistivity and high chargeability values that are visible from an approximate starting electrode position of the survey line all through to the end at depths ranged from about 40 m to 135 m.

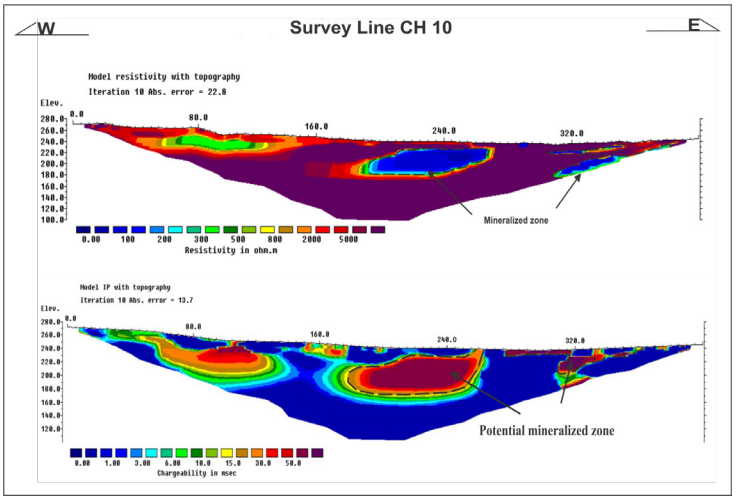

FIGURE 5. Inverted resistivity and chargeability model for the Pole - dipole electrode configuration geoelectric profile seventeen (CH 10)

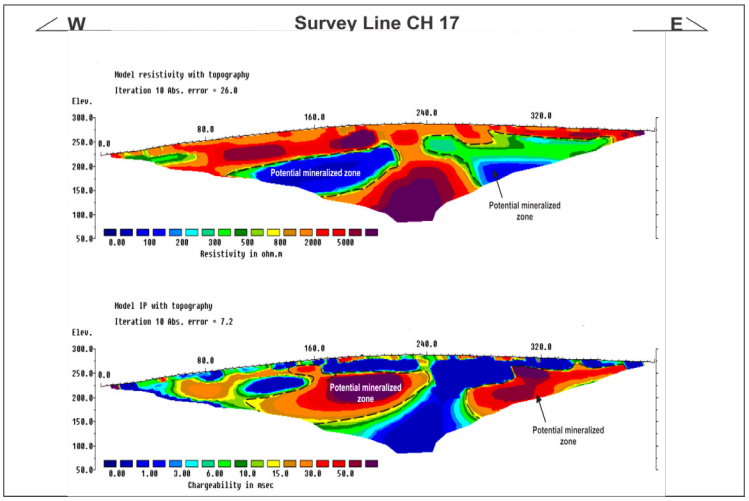

FIGURE 6. Inverted resistivity and chargeability model for the Pole - dipole electrode configuration geoelectric profile ten (CH 17)

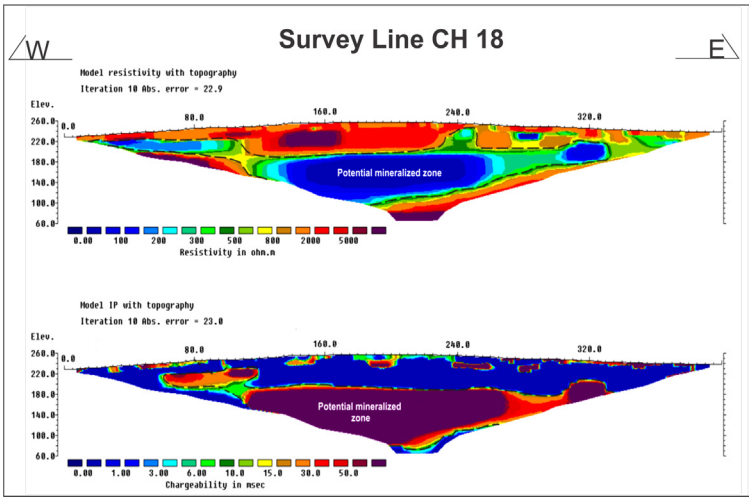

FIGURE 7. Inverted resistivity and chargeability model for the Pole - dipole electrode configuration geoelectric profile eighteen (CH 18)

All the results recorded were furthermore presented as a fence diagram to better highlighted trends of the conductive sulphide mineralization zones that hosted the hydrothermal quartz vein features along all the geoelectric survey profile lines as presented in Figure 8. The extension of the extremely low resistivity zones, i.e., typical of < 600 Ohm-m, that could be seen to be almost consistent along all the geoelectric profiles, with approximate N-S trending showed in Figure 8(a). By comparison, the well-defined regions of high chargeability values recorded (i.e., > 9.3 msec; indicated by the black dashed lines), are characterized by the same trending as that of the low resistive sulphide mineralize structures presented in Figure 8(b).

The inverted IP results recorded were combined together using their GPS coordinates to create a 3D Voxel model of high chargeability response > 9.3 msec, showed in Figure 9(a). The model generated through this method was more efficient for the characterization of the anomalous chargeability responses distribution within the maximum delineated depth of 150 m.

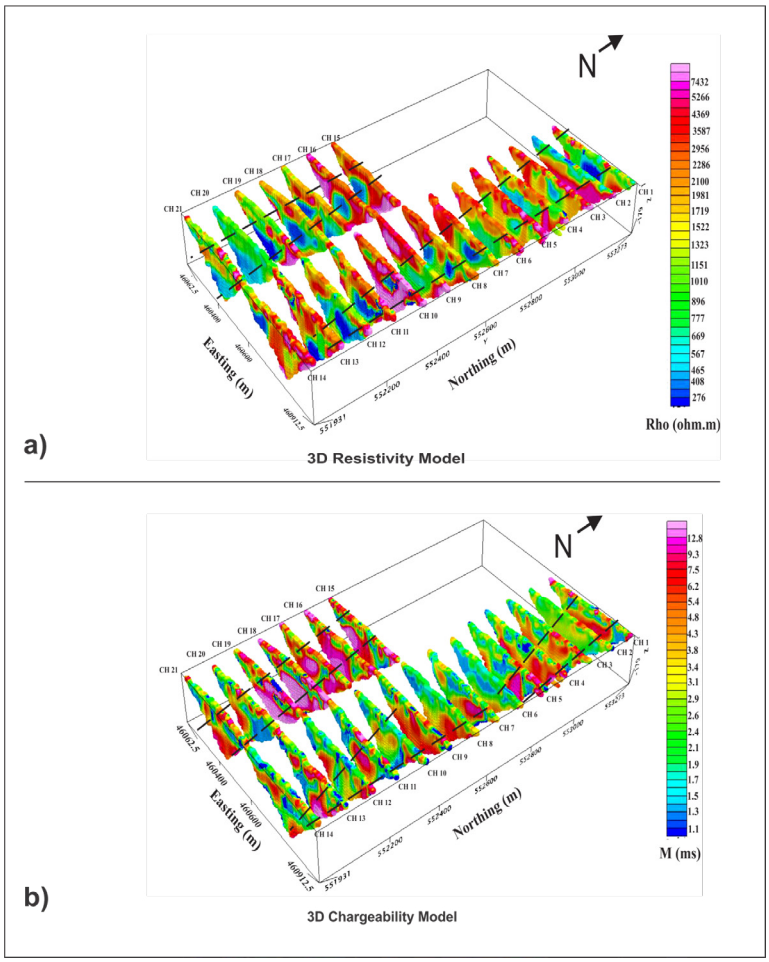

FIGURE 8. 3D model for the resistivity and chargeability showing the low resistivity /high chargeability, e.g., the black dashed lines, trending in approximately N-S directions

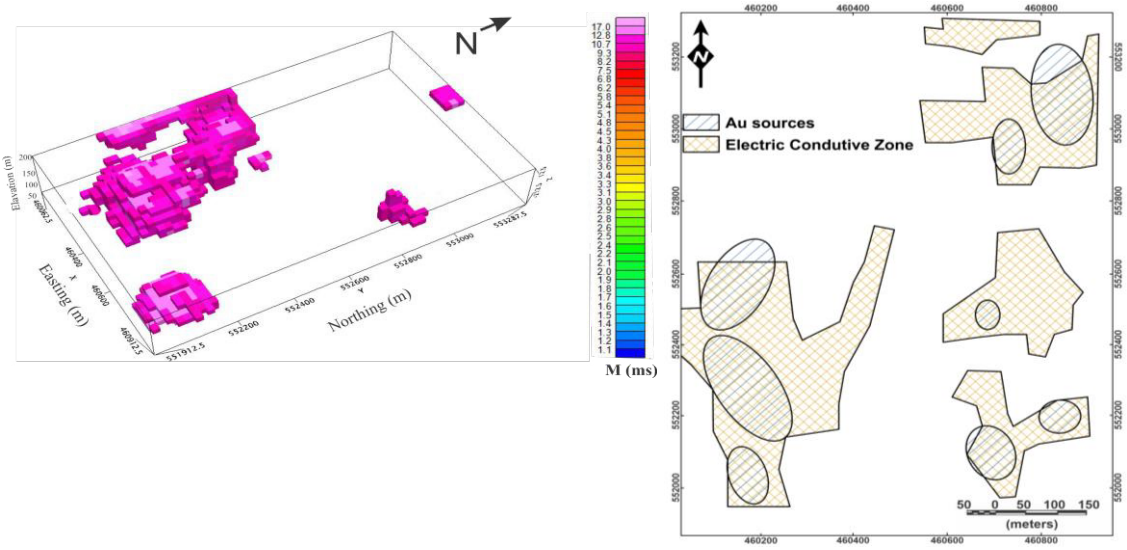

FIGURE 9. (a) A 3D voxel model for the high chargeability values showing the concentration of the polarized values along the S-W directions of the project area and (b) An integrated interpretation map for the geological and geophysical results from Figure 9(a) as obtained from the Felda Chiku 3 project area

Integrated interpretation map for the geological and the geophysical results from Figure 9(a) as obtained from the project area with the distribution and characterization of the anomalous chargeability responses within the maximum delineated depth of 150 m, is shown in Figure 9(b), which showed a correlation between the gold mineralized zones and the electric conductive zones.

RESISTIVITY AND CHARGEABILITY MAPS

Conductivity and chargeability concentration maps were created from the 2D inversion section models using the Oasis Montaj software in an attempt to correlate the anomalies of the conducting bodies. The resistivity concentration map, shown in Figure 10(a), showed zones with the low resistivity values in relation to the sulphide mineralize conductive rock bodies, ranging from about 10 - 600 Ohm-m, and spatially distributed with a delineated large-scale at the south-west regions of the study area. The other zones that delineated low resistivity values at a small-scale, were observed in the southeastern, and northern parts of the study area. Figure 10(b) shows the chargeability map of the survey area. The high chargeability zones, e.g., areas with recorded chargeability values that are greater than 8.2 msec, by comparison with the resistivity map produced, were observed to be at the same location points of the low resistivity zones, which could be interpreted as the conductive sulphide mineralize zones.

Figure 11 shows the results recorded for both the resistivity, and the IP slice maps according to the various delineated depth levels along each of the 21 Pole - dipole electrode configuration geoelectric profiles with varied resistivity from between < 276 Ohm-m, and > 17350 Ohm-m. A close observation of the resistivity map at depth of about 5 m, shows that the northern, and the southwestern parts of the study area, are mostly characterized by the smaller regions of low resistivity sulphide mineralize structures. The extension of these regions was observed to increase with depths at 107 m and 135 m, as shown in Figure 11(a), and are more visible at the depths of about 30 m and 50 m, respectively. These regions with low resistivity sulphide mineralize zones were associated with high chargeability anomalies presented in Figure 11(b), with varied chargeability values from < 1.1 msec, and > 17.0 msec.

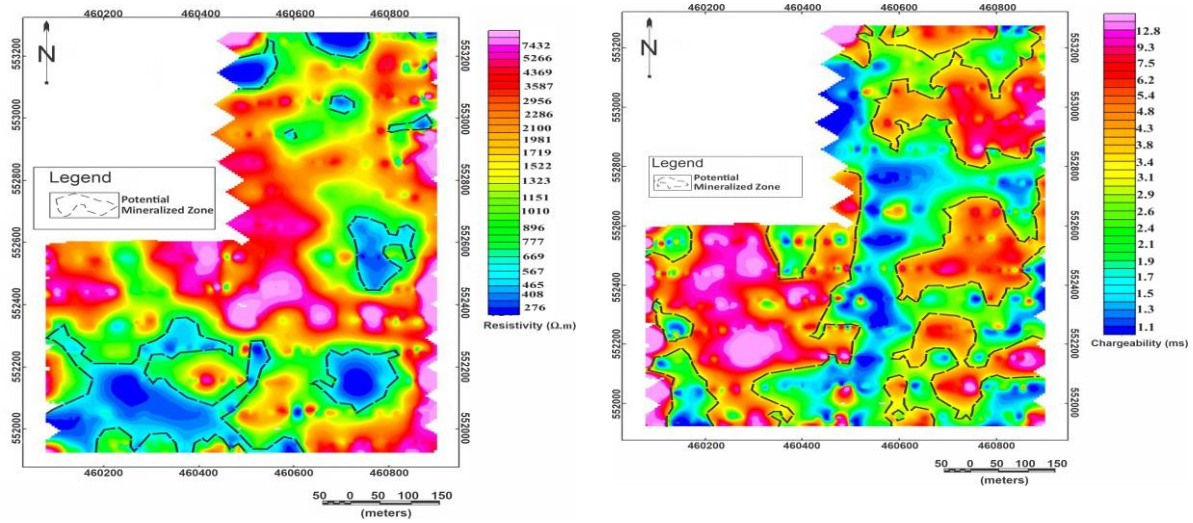

FIGURE 10. (a) Resistivity map that showed the low resistivity values, i.e., the blue region marked with dashed lines, correlating with Figure 10(b) and (b) High chargeability values, i.e., the purple region marked with dashed lines, on the Chargeability map

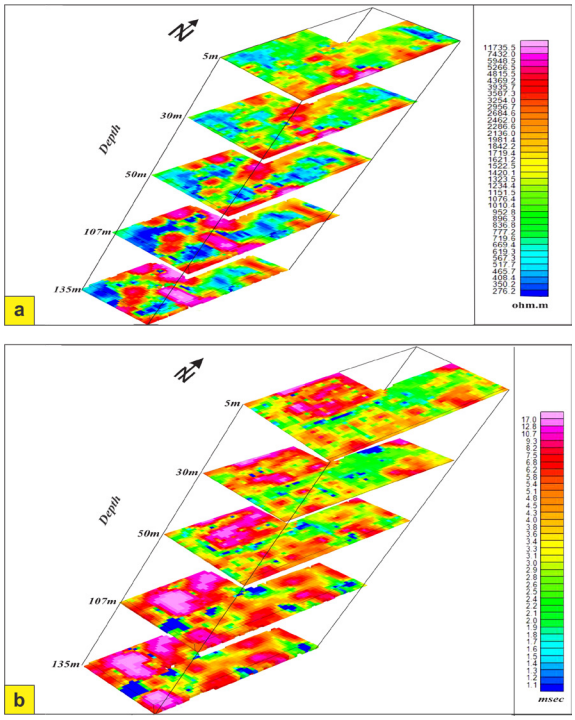

FIGURE 11. (a) Resistivity and (b) chargeability depth slice maps of the Felda Chiku 3

DISCUSSION OF RESULTS

The ERI and the IP datasets recorded in the study area facilitated the delineation of the subsurface geologic structures underlain the study region, with the resistivity maps producing the best resolution of the geoelectrical properties of the subsurface bedrocks in the area. Whilst, the IP results were used to locate zones of conductive sulphide minerals as distributed within the host rocks in the area. Analysis of the recorded ERI, and the IP pseudo-sections, produces two different geological zones of large-scale conductive sulphide minerals, and regions with low resistivity sulphide mineralize zones as delineated. The pseudo-sections generated showed a high-quality correlation among all the Twenty-one (21), geoelectrical survey profiles deployed for the research work as shown in Figures 10 and 11.

The regions that were characterized by the recorded low resistivity and high chargeability values, could be an indication of the presence of conductive sulphide minerals rock bodies, and/or weak zones. Considering the geological setting of the study area, the weak zones coincided with the shear zones at the Malaysian central gold belt (MCGB). Furthermore, the low resistivity features observed in the Felda Chiku 3 area, are likely to be caused by the shear and weathering processes of the shallow *in-situ* metamorphic rocks that are primarily made up of the lapilli tuff, the phyllites, and schist formations with the majority of the phyllites and the schist rocks, enclosing the sulphide mineralized quartz veins. This could be interpreted as the alteration shear zones that are associated with the conductive sulphide minerals, which principally comprise of the phyllites and the schist's rocks within the sheared granitoid structures.

The second sulphide mineralized zone is characterized by the high resistivity and low chargeability features that reflected the hard rock basement complex. It coincides with the geological background of the interbedded sandstone, phyllite, schist, and lapilli tuff which sometimes outcrop at the ground surface. The unweather rock units at the deeper depth are responsible for the increasing resistivity values from the near surface downwards to the bottom of the maps generated. The chargeability values recorded in this zone could be observed to be correlated with the low occurrence of the sulphide mineralization.

In addition, interpretation of the combined ERI, and IP concentration maps, shows that the spatial distributions of the zones with low resistivity and high chargeability features are well correlated and consistent with the N-S trending, which coincides with the geological information as described. The results obtained in the Felda Chiku 3 study sites proposed that the conductive features are the most promising targeted zones for followed-up drilling operations as these zones likely reflected a significant amount of the sulphide mineralization. Results from the 3D slice model depths map are helpful in predetermining of the depth of the proposed drill boreholes and delineating the gold mineralization zones in the survey area.

The normalized chargeability, which is a plot of chargeability/resistivity recorded for both the chargeability and the resistivity along a typical profile from the study area, is presented in Figure 12. Places with high and low conductive subsurface bodies, together with weathered subsurface materials and the basement are clearly demarcated. The detail survey parameters along each profile line used to generate the normalized chargeability/resistivity with an estimated maximum depth penetration are presented in Table 1. Recorded values of the IP chargeability, and RES2D were plotted using the elevation against the distance along the ground surface.

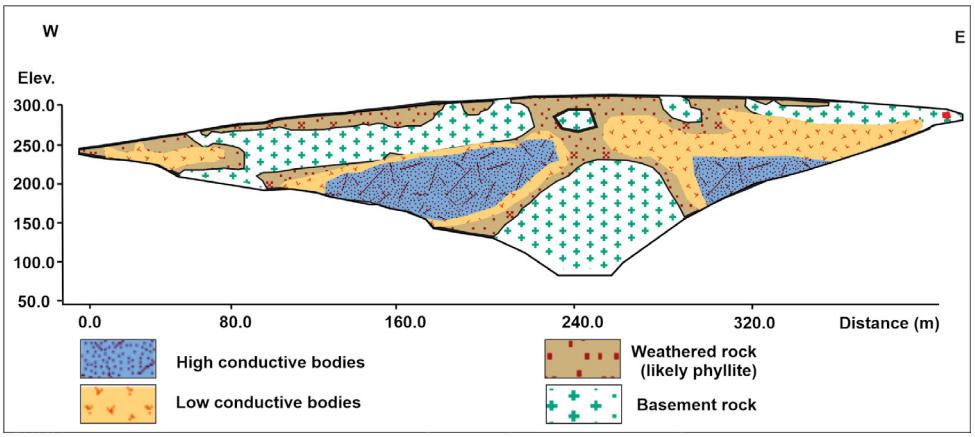

FIGURE 12. A typical normalized chargeability along W-E, i.e., chargeability/ resistivity recorded for both the chargeability and the resistivity from the Felda Chiku 3 study area

Conclusion

An integrated study involving the ERI and IP techniques, was carried out in the survey area to locate potential sulphide mineralization zones. Various geoelectric measurements were performed along several parallel geophysical survey lines. The results recorded present a good correlation between the low resistivity/high conductive values, with that of the high/low chargeability values. Hence, the presence of sulphide associated with gold mineralization in the quartz veins within the shear zones was made possible to be delineated. From the interpretation of all the geological and geophysical datasets, it could be summarized as follows. Results from the 2D resistivity and chargeability slice model generated from the pole-dipole geoelectric field datasets designated a well correlated conductive, and chargeable subsurface rock bodies that were clearly defined especially at the depths of about 25 m, and 50 m, respectively. The highly chargeability susceptible sulphide mineralization was outlined at the southwestern, the northern and southeastern parts of the Felda Chiku 3 study area. The high resistivity response could be attributed to the phyllite, sandstone, and the schist metamorphic rocks, whereas the intermediate to the high chargeability values recorded were subjected to the sulphides, or some other conductive materials that were hosted in the wall rock units. All the interpreted disseminated sulphide mineralized zones that were identified through the resistivity and chargeability signatures should be followed up by a borehole drilling programme as pinpointed on the result.

Acknowledgements

This study was jointly supported by the Ministry of Higher Education, Malaysia under Fundamental research grant No. FRGS/1/2022/WAB07/UKM/02/1 and Geo Technology Resources SDN BHD. We thank Editor-in-Chief and the reviewers of Sains Malaysiana for their constructive and helpful suggestions, which significantly improved this paper. Special thanks are due to the staff of Program Geologi, Jabatan Sains Bumi dan Alam Sekitar, Fakulti Sains dan Teknologi, Universiti Kebangsaan Malaysia for their assistance and related discussions.

References

Afiq, F.A.R., Abdul, G.R., Ailie, S.S., Rini, A.A., Afikah, R., Wan Salmi, W.H., Foong, S.Y., Muslim, A., Lee, K.E., Nguyen, X.H, Tran, V.X. & Goh, T.L. 2022. Application of a comprehensive rock slope stability assessment approach for selected Malaysian granitic rock slopes. *Sains Malaysiana* 51(2): 421-436.

Ariffin, K.S. 2012. Mesothermal lode gold deposit central belt Peninsular Malaysia. Chapter 15. In *Earth Sciences,* edited by Ahmad Dar, I. pp. 313-342. http://doi.org/10.5772/1132

Ariffin, K.S. & Hewson, N.J. 2007. Gold-related sulfide mineralization and ore genesis of the Penjom gold deposit, Pahang, Malaysia. *Resource Geology* 57(2): 149-169.

Arifin, M.H., Kayode, J.S., Ismail, M.K.I., Abdullah, A.M., Embrandiri, A., Nazer, N.S.M. & Azmi, A. 2020a. Environmental hazard assessment of industrial and municipal waste materials with the applications of RES2-D method and 3-D Oasis Montaj modeling: A case study at Kepong, Kuala Lumpur, Peninsula Malaysia. *Journal of Hazardous Materials* 406: 124282. https://doi.org/10.1016/j.jhazmat.2020.124282

Arifin, M.H., Kayode, J.S., Muhammad Khairel Izzuan Ismail, Abdul Manan Abdullah, Asha Embrandiri, Nor Shahidah Mohd Nazer & Azrin Azmi. 2020b. Data for the industrial and municipal environmental wastes hazard contaminants assessment with integration of RES2D techniques and Oasis Montaj Software. *Data in Brief* 33: 106595 https://doi.org/10.1016/j.dib.2020.106595

Arifin, M.H., Kayode, J.S., Muhammad Khairel Izzuan, Hussein Ahmed Zaid, Hamzah Hussin & S. Hanouneh, 2019. Data for the potential gold mineralization mapping with the applications of electrical resistivity imaging and induced polarization geophysical surveys. *Data in Brief* 22: 830-835. https://doi.org/10.1016/j.dib.2018.12.086

Bayrak, M. & Şenel, L. 2012. Two-dimensional resistivity imaging in the Kestelek boron area by VLF and DC resistivity methods. *Journal of Applied Geophysics* 82: 1-10. https://doi.org/10.1016/j.jappgeo.2012.03.010

Chu, L.H. & Santokh Singh, D. 1986. The nature and potential of gold mineralization in Kelantan, Peninsular Malaysia. *Bulletin of the Geological Society of Malaysia* 19: 431-440. https://doi.org/10.7186/bgsm19198632

Dahlin, T. & Zhou, B. 2004. A numerical comparison of 2D resistivity imaging with 10 electrode arrays. *Geophysical Prospecting* 52(5): 379-398.

Doyle, H.A. 1990. Geophysical exploration for gold: A review. *Geophysics* 55(2): 134-146. https://doi.org/10.1190/1.1442820

Endut, Z., Ng, T., Aziz, J.H.A. & Teh, G. 2015. Structural analysis and vein episode of the Penjom gold deposit, Malaysia: Implications for gold mineralisation and tectonic history in the central belt of Malaysia. *Ore Geology Reviews* 69: 157-173.

Flores, C. & Peralta-Ortega, S.A. 2009. Induced polarization with in-loop transient electromagnetic soundings: A case study of mineral discrimination at El Arco Porphyry Copper, Mexico. *Journal of Applied Geophysics* 68(3): 423-436.

Fon, A.N., Che, V.B. & Suh, C.E. 2012. Application of electrical resistivity and chargeability data on a GIS platform in delineating auriferous structures in a deeply weathered lateritic terrain, eastern Cameroon. *International Journal of Geosciences* 3(5): 960. http://dx.doi.org/10.4236/ijg.2012.325097

Ghani, A.A. 2009. Plutonism. In *Geology of Peninsula Malaysia,* edited by Hutchison, C. & Tan, D. Kuala Lumpur: Geological Society of Malaysia. pp. 211-231.

Goh, S.H., Teh, G.H. & Wan Fuad, W.H. 2006. Gold mineralization and zonation in the State of Kelantan. *Bulletin of the Geological Society of Malaysia* 52: 143-152. https://doi.org/10.7186/bgsm52200617

Gouet, D.H., Ndougsa-Mbarga, T., Meying, A., Assembe, S.P. & Man-Mvele Pepogo, A. 2013. Gold mineralization channels identification in the Tindikala-Boutou Area (Eastern-Cameroon) using geoelectrical (DC & IP) methods: A case study. *International Journal of Geosciences* 4(3): 643.

Haidarian Shahri, M.R., Karimpour, M.H. & Malekzadeh, A. 2010. The exploration of gold by magnetic method in Hired Area, South Khorasan, a case study. *Journal of the Earth & Space Physics* 35(4): 33-44.

Irvine, R.J. & Smith, M.J. 1990. Geophysical exploration for epithermal gold deposits. *Journal of Geochemical Exploration* 36(1-3): 375-412. https://doi.org/10.1016/0375-6742(90)90061-E

Kayode, J.S., Arifin, M.H., Basori, M.B.I. & Mohd Nawawi, M.N. 2022. Gold prospecting mapping in the Peninsular Malaysia gold belts. *Pure Appl. Geophys.* 179: 3295-3328. https://doi.org/10.1007/s00024-022-03121-w

Kayode, J.S., Arifin, M.H. & Nawawi, M. 2019. Characterization of a proposed quarry site using multi-electrode electrical resistivity tomography. *Sains Malaysiana* 48(5): 945-963. http://dx.doi.org/10.17576/jsm-2019-4805-03

Kayode, J.S., Arifin, M.H., Kamarudin, M.K.A., Hussin, A., Nordin, M.N.M. & Roslan, N. 2019. The vulnerability of the aquifer units in the flood-affected areas of the east coast Peninsula Malaysia. *Arabian Journal of Geosciences* 12(5): 146. https://doi.org/10.1007/s12517-019-4323-2

Keary, P. & Brooks, M. 1991. *An Introduction to Geophysical Exploration.* Oxford: Blackwell Scientific Publication.

Kumar, D., Rao, D.S., Mondal, S., Sridhar, K., Rajesh, K. & Satyanarayanan, M. 2017. Gold-sulphide mineralization in ultramafic-mafic-granite complex of Jashpur, Bastar Craton, Central India: Evidences from geophysical studies. *Journal of the Geological Society of India* 90(2): 147-153.

Lenhare, B.D. & Moreira, C.A. 2020. Geophysical prospecting over a meta-ultramafic sequence with indicators of gold mineralization in Rio Grande do Sul State, Southernmost Brazil. *Pure and Applied Geophysics* 177: 5367-5383. https://doi.org/10.1007/s00024-020-02559-0

Li, B., Jiang, S.Y., Zou, H.Y., Yang, M. & Lai, J.Q. 2015. Geology and fluid characteristics of the Ulu Sokor Gold Deposit, Kelantan, Malaysia: Implications for ore genesis and classification of the deposit. *Ore Geology Reviews* 64: 400-424.

Loke, M. 2001. Constrained time-lapse resistivity imaging inversion. *Symposium on the Application of Geophysics to Engineering and Environmental Problems Proceedings:* EEM7-EEM7. https://doi.org/10.4133/1.2922877

Loke, M.H. 2016. *Tutorial: 2-D and 3-D Electrical Imaging Surveys*. http://www.geotomosoft.com

Macdonald, S. 1967. *The Geology and Mineral Resources of North Kelantan and North Trengganu.* Geological Survey Headquaters.

Makoundi, C., Zaw, K., Large, R.R., Meffre, S., Lai, C.K. & Hoe, T.G. 2014. Geology, geochemistry and metallogenesis of the Selinsing gold deposit, central Malaysia. *Gondwana Research* 26(1): 241-261.

Marescot, L., Monnet, R. & Chapellier, D. 2008. Resistivity and induced polarization surveys for slope instability studies in the Swiss Alps. *Engineering Geology* 98(1-2): 18-28.

Mashhadi, S.R. & Ramazi, H. 2018. The application of resistivity and induced polarization methods in identification of skarn alteration haloes: A case study in the Qale-Alimoradkhan area. *Journal of Environmental and Engineering Geophysics* 23(3): 363-368. https://doi.org/10.2113/JEEG23.3.363

Mashhadi, S.R., Nikfarjam, M. & Mehrnia, A.K. 2020, Reinterpretation of resistivity and induced polarization data to explore gold mineralization zones at Zarzima prospect, Iran. *Acta Geologica Slovaca* 12(1): 15-22.

Metcalfe, I. 2013. Gondwana dispersion and asian accretion: Tectonic and palaeogeographic evolution of eastern tethys. *Journal of Asian Earth Sciences* 66: 1-33.

Metcalfe, I. 2000. The Bentong-Raub Suture Zone. *Journal of Asian Earth Sciences* 18(6): 691-712.

Moon, C., Whateley, K. & Evans, A. 2006. *Introduction to Mineral Exploration.* Oxford: Blackwell Publishing.

Moreira, C.A., Casagrande, M.F.S. & Borssatto, K. 2020. Analysis of the potential application of geophysical survey (induced polarization and DC resistivity) to a long-term mine planning in a sulfide deposit. *Arabian Journal of Geosciences* 13(20): 1-12. https://doi.org/10.1007/s12517-020-06096-x

Moreira, C.A., Borssatto, K., Ilha, L.M., Santos, S.F.D. & Rosa, F.T.G. 2016. Geophysical modeling in gold deposit through DC resistivity and induced polarization methods. *REM-International Engineering Journal* 69(3): 293-299. https://doi.org/10.1590/0370-44672016690001

Mostafaei, K. & Ramazi, H.R. 2018. 3D model construction of induced polarization and resistivity data with quantifying uncertainties using geostatistical methods and drilling (Case study: Madan Bozorg, Iran). *Journal of Mining and Environment* 9(4): 857-872. DOI. 10.22044/jme.2018.6852.1516

Nazaruddin, D.A., Fadilah, N.S.M., Zulkarnain, Z., Omar, S.a.S. & Ibrahim, M.K.M. 2014. Geological studies to support the tourism site: A case study in the Rafflesia trail, near Kampung Jedip, Lojing Highlands, Kelantan, Malaysia. *International Journal of Geosciences* 5(8): 835.

Pour, A.B. & Hashim, M. 2015. Structural mapping using palsar data in the Central Gold Belt, Peninsula Malaysia. *Ore Geology Reviews* 64: 13-22.

Pour, A.B., Hashim, M., Makoundi, C. & Zaw, K. 2016. Structural mapping of the Bentong-Raub suture zone using palsar remote sensing data, Peninsula Malaysia: Implications for sediment-hosted/orogenic gold mineral systemsec exploration. *Resource Geology* 66(4): 368-385.

Power, C., Tsourlos, P., Ramasamy, M., Nivorlis, A. & Mkandawire, M. 2018. Combined DC resistivity and induced polarization (DC-IP) for mapping the internal composition of a mine waste rock pile in Nova Scotia, Canada. *Journal of Applied Geophysics* 150: 40-51. https://doi.org/10.1016/j.jappgeo.2018.01.009

Reynolds, J.M. 2011. *An Introduction to Applied and Environmental Geophysics*. New York: John Wiley & Sons.

Salarian, S., Asghari, O., Abedi, M. & Alilou, S.K. 2019. Geostatistical-based geophysical model of electrical resistivity and chargeability to image Cu mineralization in Ghalandar deposit, Iran. *International Journal of Mining Geo-Engineering* 54-2: 153-160.

Sevastjanova, I., Clements, B., Hall, R., Belousova, E.A., Griffin, W.L. & Pearson, N. 2011. Granitic magmatism, basement ages, and provenance indicators in the Malay Peninsula: Insights from detrital zircon U–Pb and Hf-Isotope data. *Gondwana Research* 19(4): 1024-1039.

Sharma, P.V. 1997. *Environmental and Engineering Geophysics*. Cambridge: Cambridge University Press.

Smith, R.C. & Sjogren, D.B. 2006. An evaluation of electrical resistivity imaging (ERI) in quaternary sediments, Southern Alberta, Canada. *Geosphere* 2(6): 287-298.

Sono, P., Nthaba, B., Shemang, E.M., Kgosidintsi, B. & Seane, T. 2020. An integrated use of induced polarization and electrical resistivity imaging methods to delineate zones of potential gold mineralization in the Phitshane Molopo area, Southeast Botswana. *Journal of African Earth Sciences* 2020: 104060. https://doi.org/10.1016/j.jafrearsci.2020.104060

Spitzer, K. & Chouteau, M. 2003. A DC resistivity and IP borehole survey at the Casa Berardi gold mine in Northwestern Quebec. *Geophysics* 68(2): 453-463. https://doi.org/10.1190/1.1567221

Sultan, S.A., Mansour, S.A., Santos, F.M. & Helaly, A.S. 2009. Geophysical exploration for gold and associated minerals, case study: Wadi El Beida area, South Eastern Desert, Egypt. *Journal of Geophysics and Engineering* 6(4): 345-356. https://doi.org/10.1088/1742-2132/6/4/002

Sumner, J. 1976. *Principles of Induced Polariration for Geophysical Exploration*. Amsterdam: Elsevier Scientific Publishing Company.

Tagwai, M.G., Jimoh, O.A., Ariffin, K.S. & Abdul Razak, M.F. 2019. Investigation based on quantified spatial relationships between gold deposits and ore genesis factors in northeast Malaysia. *Journal of Spatial Science* 66(2): 229-252. https://doi.org/10.1080/14498596.2019.1606742

Telford, W.M., Geldart, L. & Sheriff, R.E. 1990. *Applied Geophysics.* 2nd ed. Cambridge: Cambridge University Press.

Upadhyay, A., Singh, A., Panda, K.P. & Sharma, S.P. 2020. Delineation of gold mineralization near Lawa Village, North Singhbhum Mobile Belt, India, using electrical resistivity imaging, self-potential and very low frequency methods. *Journal of Applied Geophysics* 172: 103902. https://doi.org/10.1016/j.jappgeo.2019.103902

Vieira, L.B., Moreira, C.A., Côrtes, A.R. & Luvizotto, G.L. 2016. Geophysical modeling of the manganese deposit for induced polarization method in Itapira (Brazil). *Geofísica Internacional* 55(2): 107-117.

Wynn, J.C. & Grosz, A.E. 2000. Induced polarization - A tool for mapping titanium-bearing placers, hidden metallic objects, and urban waste on and beneath the seafloor. *Journal of Environmental & Engineering Geophysics* 5(3): 27-35. https://doi.org/10.4133/JEEG5.3.27

Yao, K., Pradhan, B. & Idrees, M.O. 2017. Identification of rocks and their quartz content in Gua Musang goldfield using advanced spaceborne thermal emission and reflection radiometer imagery. *Journal of Sensors* 2017: 6794095. https://doi.org/10.1155/2017/6794095

Yeap, E. 1993. Tin and gold mineralizations in Peninsula Malaysia and their relationships to the tectonic development. *Journal of Southeast Asian Earth Sciences* 8(1-4): 329-348.

Yusoff, A.F., Abdul Aziz, J.H. & Roselee, M.H. 2022. Mineralogy and geochemistry of gold mineralization at southern part of Ulu Sokor gold deposit, Kelantan, Malaysia. *Sains Malaysiana* 51(12): 3865-3877.

Zhang, Y., Chu, F., Li, Z., Dong, Y., Wang, H., Li, X. & Long, J. 2020. Gold enrichment in hydrothermal sulfides from the Okinawa Trough: An *in-situ* LA-ICP-MSEC study. *Ore Geology Reviews* 116: 103255. https://doi.org/10.1016/j.oregeorev.2019.103255

*Corresponding author; email: hariri@ukm.edu.my